International Journal of Neural Systems (2021) 2150052 (19 pages)

DOI: 10.1142/S0129065721500520

World Scientific
www.worldscientific.com

Corticomuscular and Intermuscular Coupling in Simple Hand Movements to Enable a Hybrid Brain–Computer Interface

Emma Colamarino[*,†,‡], Valeria de Seta[*,†,§], Marcella Masciullo[†,¶], Febo Cincotti[*,†,‖], Donatella Mattia[†,**], Floriana Pichiorri[†,††] and Jlenia Toppi[*,†,‡‡]

[*]*Department of Computer, Control and Management Engineering Sapienza University of Rome, Via Ariosto 25, Rome 00185, Italy*

[†]*Fondazione Santa Lucia IRCCS, Via Ardeatina 306-354, Rome 00179, Italy*

[‡]*emma.colamarino@uniroma1.it*
[§]*deseta@diag.uniroma1.it*
[¶]*m.masciullo@hsantalucia.it*
[‖]*cincotti@diag.uniroma1.it*
[**]*d.mattia@hsantalucia.it*
[††]*f.pichiorri@hsantalucia.it*
[‡‡]*jlenia.toppi@uniroma1.it*

Accepted 27 Aug 2021
Published Online

Hybrid Brain–Computer Interfaces (BCIs) for upper limb rehabilitation after stroke should enable the reinforcement of "more normal" brain and muscular activity. Here, we propose the combination of corticomuscular coherence (CMC) and intermuscular coherence (IMC) as control features for a novel hybrid BCI for rehabilitation purposes. Multiple electroencephalographic (EEG) signals and surface electromyography (EMG) from 5 muscles per side were collected in 20 healthy participants performing finger extension (Ext) and grasping (Grasp) with both dominant and non-dominant hand. Grand average of CMC and IMC patterns showed a bilateral sensorimotor area as well as multiple muscles involvement. CMC and IMC values were used as features to classify each task versus rest and Ext versus Grasp. We demonstrated that a combination of CMC and IMC features allows for classification of both movements versus rest with better performance (Area Under the receiver operating characteristic Curve, AUC) for the Ext movement (0.97) with respect to Grasp (0.88). Classification of Ext versus Grasp also showed high performances (0.99). All in all, these preliminary findings indicate that the combination of CMC and IMC could provide for a comprehensive framework for simple hand movements to eventually be employed in a hybrid BCI system for post-stroke rehabilitation.

Keywords: Hybrid brain–computer interface; electroencephalography; electromyography; corticomuscular coherence; intermuscular coherence; upper limb.

1. Introduction

Brain–Computer Interfaces (BCIs) have successfully been employed to address upper limb motor rehabilitation after stroke.[1,2] Most BCIs targeting upper limb functional motor recovery exploit brain signals (most commonly recorded via electroencephalography, EEG)[3] to control visual or proprioceptive feedbacks/effectors[4,5] which ultimately aim at reinforcing "more normal" brain activation by closing the sensorimotor loop.[6–8] However, residual or recovered muscular activity can be monitored along the rehabilitation process and guided towards "more normal" movement patterns to achieve maximum possible functional regain.[9] It is well known that the regaining of motor function after stroke is characterized by several changes in muscular activation

[‡‡]Corresponding author.

patterns, such as motor overflow,[10] co-activation of agonist and antagonist muscles and spasticity.[11–15] Rehabilitation approaches should be designed to counteract these maladaptive changes.[16] Currently available rehabilitative BCIs mostly overlook these aspects along with the training protocols, if at all restricting their assessment within the evaluation phases (e.g. to determine efficacy).

Hybrid BCIs include peripheral signals such as those derived from electromyography (EMG) as a control feature.[17] These have mostly been developed to improve the classification performance of the system e.g. in assistive BCIs,[17–19] with little or no focus on which properties of the EMG signals should be considered in a rehabilitative context. Applications of hybrid BCIs for motor rehabilitation after stroke are still limited.[20,21] The EMG features employed in these few studies include amplitude estimates, such as the envelope and other features extracted from the surface EMG signal (e.g. the waveform length,[22] the mean of the absolute value, the variance, the root-mean-square error and the logarithm of the variance of the EMG signal[23]). However, there is no consensus on which movement-related features should be encouraged (or discouraged) within a BCI training to pursue physiological muscular activation patterns. Ideally, hybrid BCI systems specifically developed for hand motor rehabilitation should allow to train both brain and peripheral activity in a top-down framework,[24] in which volition, that is brain control over muscular activation, is reinforced together with correct muscular activation patterns.[25]

To address this approach in designing hybrid BCI for motor rehabilitation, we propose the combination of corticomuscular coherence (CMC) and intermuscular coherence (IMC) as novel features to control hybrid BCIs. The CMC is a measure of synchronization between central and peripheral activation. Stroke- related CMC studies have shown alterations in both the acute and chronic phases[26–29]; furthermore, changes have been correlated with functional recovery.[30] The IMC provides information about the common corticospinal drive among different muscles and has been employed to investigate intermuscular coordination during upper limb motor tasks in healthy participants.[31,32] In stroke subjects, IMC provides information on the pathophysiological basis of altered muscular patterns related e.g. to spasticity.[10] It has been shown that both CMC[33] and IMC[34] can be modulated in a neurofeedback/biofeedback training paradigm.

The combination of information encoded in CMC and IMC would enable a hybrid BCI to reinforce volitional control of those movement attempts that most resemble physiological muscular activation patterns, thereby lessening the probability to facilitate maladaptive motor re-learning.

In this study, we first explored both CMC and IMC in healthy participants performing simple hand movements such as finger extension and grasping. These tasks are the most used in BCI-based rehabilitative contexts.[4,5,35] Although some studies in both healthy and stroke participants have employed CMC as a BCI control feature,[33,36] the combined use of CMC-IMC for hybrid rehabilitative BCIs has not been conceived yet.

It is well known that brain activity and connectivity patterns are widely altered after stroke[37] and such changes involve brain areas distant from the lesion, both ipsi and contralateral to the lesion itself. The muscular patterns are also altered after stroke resulting in excess activation of muscles other than the target one (motor overflow, coactivation of agonists and antagonists and even bilateral involvement[38,39]). Therefore, we estimated CMC and IMC values from multiple EEG and EMG electrodes rather than considering only few predetermined scalp electrodes and movement target muscles.[29,30,36] This multichannel approach returned EEG-EMG and EMG-EMG synchronization pairs as a comprehensive functional connectivity pattern for each tested movement. The performances of CMC and IMC as features to classify simple hand motor tasks versus rest or different tasks against each other were evaluated.

This signal processing framework will contribute to the design of a novel hybrid BCI system for upper limb motor rehabilitation in stroke subjects, providing the necessary knowledge on (i) how multimodal features should be defined for successful detection of correct (i.e. “close to normal”) movement to be volitionally controlled via BCI, and eventually implemented for the online processing, (ii) the inter-subject and intra-subject variability to be taken into account when approaching the variety of movement impairment in stroke population.

2. Materials and Methods

2.1. *Participants and experimental protocol*

Twenty healthy volunteers (9 females/11 males, age 27.8 ± 2.4 years), all right-handed and with no history of neuromuscular disorders, were enrolled in the study. All participants were informed about the experimental protocol and gave their informed written consent to the study. The study was approved by the ethics board of the IRCCS Fondazione Santa Lucia, Rome, Italy (Prot. CE/PROG. 730).

During the experiment, participants were seated in a comfortable chair with their forearms on the armrests. Visual cues were presented on a screen facing them. Participants were instructed to perform four movements: finger extension (Ext) and grasping (Grasp), with either the right (R) and left (L) hand. The experiment was administered in two sessions including 4 blocks (one per movement: ExtR, ExtL, GraspR, GraspL) of 30 trials each. We set an inter-block break of 1 min and an inter-session break of 10 min. The block sequence was randomized inter- and intra-sessions. The total trial duration was 7 s with an inter-trial interval of 3.5 s. Each trial began with a cursor appearing at the bottom of the screen, moving toward the top at constant velocity on a vertical line, reaching the top of the screen at the end of the trial. The screen was split into two vertically stacked regions with different background color (black/green for the bottom/top regions, respectively), so that the moving cursor would cross the boundary between the regions exactly 3 s after the trial's start (Fig. 1). The moving cursor provided the participants with a visual cue of the timing of the tasks: participants were instructed to rest in the first 3 s of the trial (cursor in the black region) and to perform the task along the remaining 4 s (cursor on the green region). The task consisted of a gradual extension or flexion of their right- or left-hand fingers, spanning across the final 4 s of each trial.

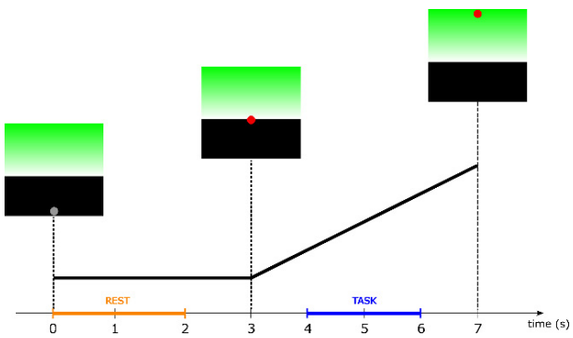

Fig. 1. (Color online) Timeline of the experiment with details on the screen shown to the participant. The orange and the blue lines show the time intervals selected for the analysis of rest ([0 2]s) and task ([4 6]s), respectively.

This instruction was given to reduce the inter-subject and intra-subject variability in executing the motor tasks. Furthermore, such gradual/slow execution of finger extension/grasping was chosen as more suitable keeping in mind the target stroke population with different degrees of motor impairment.

2.2. *EEG and EMG data collection*

Electroencephalographic (EEG) and electromyographic (EMG) signals were simultaneously collected with a sampling frequency of 2400 Hz by means of the g.HIamp amplifier (g.tec medical engineering GmbH Austria). Scalp EEG potentials were collected from thirty-one passive electrodes assembled on an electrode cap placed above the sensorimotor area according to an extension of the International 10–20 system (FC5, FC3, FC1, FCz, FC2, FC4, FC6, C5, C3, C1, Cz, C2, C4, C6, CP5, CP3, CP1, CPz, CP2, CP4, CP6, P5, P3, P1, Pz, P2, P4, P6, PO3, POz, PO4). Potentials were referenced to the linked earlobes and grounded to the left mastoid. The contact impedance of each electrode was kept below 5kΩ. The EMG data were collected from 10 muscles of the upper limbs (5 per side) namely: extensor digitorum (ED), flexor digitorum superficialis (FD), triceps (TRI), biceps brachii (BIC) and lateral deltoid (DELT). EMG sensors were placed according to the guidelines reported in Barbero *et al.*[40] For each muscle, two surface Ag/AgCl electrodes, 10 mm diameter, were placed at 20 mm inter-electrode distance on the center of the muscle belly, in the direction of the muscle fibers, according to the SENIAM recommendations.[41] We minimized crosstalk between forearm muscles during electrode placement and tested it by the execution of specific movements associated with the muscles. The quality of EEG and EMG signals was visually checked prior to beginning the measurements and continuously monitored afterwards. Three maximum voluntary contractions (MVCs) lasting 5 s were

recorded for each muscle[42,43] at the beginning of the experiment.

2.3. *Data analysis*

Figure 2 shows the flow chart illustrating the methodological steps of the analyses presented.

2.3.1. *EEG and EMG data pre-processing*

Vision Analyzer 1.05 software (Brain Products GmbH, Gilching, Germany) was used to pre-process the data. EEG and EMG signals were downsampled to 1000 Hz after an appropriate filtering to avoid aliasing. EEG and EMG signals were band-pass filtered with a Butterworth zero-phase filter in the range 3–100 Hz and 3–500 Hz, respectively. A notch filter at 50 Hz was applied to remove power-line interference on both signals. Continuous traces were segmented in 7 s epochs, comprising the 3 s of rest and the 4 s of motor execution. Trials with EEG signals exceeding in absolute value the amplitude of 100 μV and trials contaminated by muscular artifacts were rejected. All EEG and EMG trials were visually inspected to identify artifacts. Following this assessment, three participants were excluded from further analysis due to artifacts in more than 50% of trials. EEG signals were re-referenced according to the common average reference. The following analyses were performed using custom code developed in Matlab R2019a (The MathWorks, Inc., Natick, Massachusetts, USA).

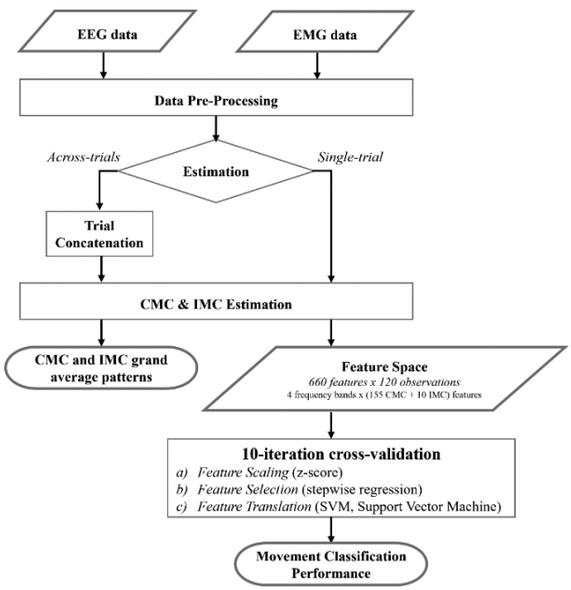

Fig. 2. Flow chart illustrating the methodological steps of the analyses.

2.3.2. *Assessment of muscle activation*

Two time intervals of interest lasting 2 s were selected for the CMC and IMC analysis according to the muscle activation level: (i) a rest interval, from 0 s to 2 s, and (ii) a task interval, from 4 s to 6 s with respect to the trial start (see Fig. 1). To verify that participants showed a stable and predictable muscle activation in these windows, we computed the EMG activation as follows. The root-mean-square (RMS) of EMG signal on the target muscle for each trial (flexor digitorum muscle for grasping movements, extensor digitorum muscle for finger extension movements) was computed on windows of 0.15 s length sliding across the whole trial duration and on the three MVC repetitions of the corresponding muscle. The EMG activation was expressed as percent of the ratio between the RMS in each short window of the trial and the maximum RMS among the three corresponding MVC repetitions (%MVC). The activation level values, expressed as %MVC, were finally averaged across all time points belonging either to the rest or the task intervals, and across trials (EMG activation level).

2.3.3. *Coherence estimation*

The magnitude squared coherence values between EEG and EMG signals, i.e. CMC, or between EMG signals, i.e. IMC, were computed in the range 8–100 Hz.

Corticomuscular coherence

The CMC values were computed as

$$\mathrm{CMC}_{xy}(f_j) = |S_{xy}(f_j)|^2 \tag{1}$$

$$S_{xy}(f_j) = \frac{1}{n}\sum_{i=1}^{n} X_i(f_j)Y_i^*(f_j), \tag{2}$$

where $S_{xy}(f_j)$ represents the cross-power spectrum between the EEG signal x and the EMG signal y at a given frequency f_j, estimated using the Welch periodogram method with a Hann window. The

length and overlap of the periodogram windows were tailored to the specific aim of the subsequent analysis (see below). EMG signals were rectified before entering in the CMC computation.[44]

We used the absolute square value of the cross-spectrum (as in 1) as measure of EEG-EMG synchronization, instead of the classical coherence formulation.[45] This approach prevents, in fact, the detection of false positives in CMC when the muscle activation level is around 0, as observed in the rest time interval of our experiment.[46] To be consistent with IMC analysis and previous literature, we will refer to the corticomuscular cross-spectrum by maintaining the acronym CMC and the designation of coherence.

Intermuscular coherence

Intermuscular coherence was computed between pairs of unrectified EMG signals recorded from muscles of the same side (10 pairs of ipsilateral muscles). The IMC values were computed as[47]

$$\mathrm{IMC}_{xy}(f_j) = \frac{|S_{xy}(f_j)|^2}{|S_{xx}(f_j)| \cdot |S_{yy}(f_j)|}, \tag{3}$$

where $S_{xy}(f_j)$ represents the cross-power spectrum between the EMG signals x and y and $S_{xx}(f_j)$ and $S_{yy}(f_j)$ are the auto-spectra of x and y, respectively. Cross- and auto-spectra were computed according to Welch periodogram with Hann window as described above for the CMC formula.

Across-trials and single-trial estimations

CMC/IMC values were estimated for each participant, movement (ExtR, ExtL, GraspR, or GraspL), and interval of interest (task, rest). Two different procedures were followed for the CMC/IMC estimation (across-trials or single-trial approaches), differing in how the periodogram windows were defined and averaged, serving different purposes in the downstream analysis. In the across-trials approach (periodogram window length of 1 s with 0% overlap) we estimated a single CMC/IMC spectrum from all trials in the dataset of a single participant for each EEG-EMG/EMG-EMG pair, in order to have an average CMC/IMC pattern for each participant to be included in the grand average (see Statistical analysis, section: CMC and IMC grand average patterns).

Before computing the average IMC pattern for each participant, the significance of non-zero IMC values were assessed[47] by comparing them to the chance level defined by the equation[48]

$$\mathrm{CL}(\alpha) = 1 - (1-\alpha)^{\frac{1}{n-1}}, \tag{4}$$

where n is the number of windows of the signals used in the spectra estimation. The significance level was set to $\alpha = 0.01$ and corrected according to the False Discovery Rate procedure, FDR.[49] Values below $\mathrm{CL}(\alpha)$ were set to zero. In the single-trial approach (periodogram window length of 0.125 s with 50% overlap), we estimated a CMC/IMC spectrum for each trial in the dataset, in order to have different observations of CMC/IMC patterns for each participant to be used as features of a classifier discriminating task versus rest or different movements among each other (see paragraph Movement classification).

Characteristic frequencies

To select specific frequencies in which CMC and IMC are modulated by a specific task, we divided the frequency spectrum into four bands: alpha (8–12 Hz), beta (13–30 Hz), gamma (31–60 Hz) and high frequencies (HF, 61–100 Hz). In each band we identified a characteristic frequency f_* as the frequency in which $\mathrm{CMC}_{xy}(f_j)$ (or $\mathrm{IMC}_{xy}(f_j)$) showed the highest value, for all f_j in the band. The characteristic frequency was specific for each pair of signals x and y, thus for each movement type (Ext and Grasp) and in each band we obtained a set of 310 characteristic frequencies for the CMC_{xy} (31 EEG $\times$ 5 EMG from muscles ipsilateral to the task side $\times$ 2 sides) and a set of 20 characteristic frequencies for the IMC_{xy} (the number of pairs among 5 EMG signals from muscles ipsilateral to the task side $\times$ 2 sides). As for "inactive" muscles, characteristic frequencies that were determined when the xy pair included a muscle ipsilateral to the movement (e.g. right DELT during GraspR) were also used for the same xy pair when the movement was contralateral to the muscle (e.g. right DELT during GraspL). Analyses of the rest interval borrowed the characteristic frequencies of the matching task interval. In subsequent analyses, only CMC/IMC values taken at the characteristic frequencies are considered.

2.3.4. *Movement classification*

A single-subject binary classification model was trained to evaluate the performance of CMC and IMC values to discriminate task versus rest intervals for each movement. CMC and IMC values from single trials were merged into a feature vector containing, therefore, CMC values from all possible EEG-EMG pairs and IMC values from all possible EMG-EMG pairs for each frequency band (CMC + IMC approach). Only pairs including muscles ipsilateral to the movement (e.g. the 5 muscles of the right upper limb in ExtR or GraspR) were included in the feature vector. Thus, the feature space was 660-dimensional: 620 CMC features (31 EEG channels × 5 EMG channels × 4 frequency bands) and 40 IMC features (10 pairs among 5 EMG channels × 4 frequency bands). For each movement and participant, the dataset consisted of 120 observations (60 trials × 2 intervals i.e. task and rest).

Feature scaling (z-score standardization) was applied to the dataset to take into account differences among types of features. A feature selection algorithm based on the stepwise regression[50] with an empty initial model was applied to reduce the dimensionality of the feature space before building the classification model. The results of this feature reduction process also served to assess the subset of features most relevant to classification (see below). A support vector machine classifier with linear kernel[36] was used as classification model on the reduced features space. A 10-iteration cross-validation was applied to evaluate the classification performances. In each iteration, 70% and 30% of the observations were used as training and testing dataset, respectively.

Two CMC + IMC more models (Ext-Grasp classifiers) were considered to assess whether CMC and IMC features can discriminate different movement types. Only features from task intervals of two ipsilateral movement types were included in each model (one model per side), thus discriminating either GraspR versus ExtR or GraspL versus ExtL classes.

In order to disentangle the role of each feature type (CMC or IMC) in the movement discrimination, the single-subject binary classification Task versus Rest and Ext versus Grasp was repeated considering CMC and IMC values as features separately (CMC and IMC approaches).

Four different metrics were computed to evaluate the performance of all classification models: (i) the area under the curve (AUC) of the Receiver Operating Characteristic (ROC) curve,[51] (ii) the accuracy, (iii) the specificity and (iv) the sensitivity of the classifier.

The subset of features selected by the stepwise regression was analyzed to identify the most recurrent EEG-EMG and EMG-EMG pairs used in the classification models. We counted the number of times a specific channel pair was selected across participants and cross-validation iterations irrespectively of the frequency band they corresponded to.

2.3.5. *Statistical analysis*

CMC and IMC grand average patterns

Each movement was described by a coherence pattern as result of a grand average analysis computed on CMC/IMC values across participants.

For each movement type, frequency band and channel pair we applied a paired sample t-test (across participants, $N = 17$) using as independent variable the interval (task versus rest) and as dependent variable the CMC/IMC values computed in the across-trials procedure. The significance level was set to 0.05. FDR was used to control family-wise error rate.

We will interpret significant differences as a marker of relevance of a specific pair/band in the execution of a specific movement.

Classification performance evaluation

To investigate the effect of the side and type of movement on the performance of task-rest classifiers, we performed a two-way repeated measures analyses of variance (ANOVA) considering as within main factors the MOVEMENT (2 levels: Ext, Grasp) and the SIDE (2 levels: right, left) and as dependent variable the AUC value.

To evaluate whether the discriminability between grasping and extension movements depends on the side, the resulting AUC values were analyzed by means of a paired t-test with significance threshold equal to 0.05.

Performances obtained by the combination of CMC and IMC features and CMC and IMC features alone were statistically compared using a one-way repeated measures ANOVA. We used AUC values as dependent variable and the features type

(CMC, IMC, CMC + IMC) as within factor. The same analysis was repeated for each movement and side in the task versus rest classification and for each side in the Ext versus Grasp classification.

The statistical significance level for all tests was set to $p < 0.05$ and the Tukey post-hoc analysis was performed to assess differences among pairs.

3. Results

3.1. *Assessment of muscle activation*

The EMG activation levels in the task interval (mean ± SE across participants, $N = 17$) were 9.5 ± 0.9 %MVC and 9.9 ± 1.0 %MVC for the extensor digitorum muscle in ExtR and ExtL, respectively, and 5.5 ± 0.9 %MVC and 6.3 ± 1.2 %MVC for the flexor digitorum muscle in GraspR and GraspL, respectively. The activation levels in the rest interval (mean ± SE across participants, $N = 17$) were 1.3 ± 0.1 %MVC and 1.3 ± 0.2 %MVC for the extensor digitorum muscle in ExtR and ExtL, respectively and 1.8 ± 0.3 %MVC and 2.5 ± 0.8 %MVC for the flexor digitorum muscle in GraspR and GraspL, respectively.

3.2. *CMC and IMC grand average patterns*

Figures 3 and 4 show the grand average CMC (panels (a) and (c)) and IMC (panels (b) and (d)) patterns observed for the right and left finger extension and grasping, respectively. As expected for a healthy experimental group, no significant CMC and IMC values were observed for the side contralateral to the movement.

As for right and left Ext movements (Fig. 3), we found the highest CMC values for connections involving mainly the target muscle (ED) and most of the bilateral sensorimotor EEG electrodes, in alpha and beta bands. At higher frequency bands (gamma and HF), CMC values were lower and less muscle specific. We also found that the left Ext movement (non-dominant hand; left hand, Fig. 3(c)) was characterized by EEG-EMG connections involving mainly the target ED muscle and other proximal muscles (e.g. deltoid), whereas the same movement executed with the dominant hand (right hand, Fig. 3(a)) showed connections also with the antagonist FD (across all frequency bands). As for the IMC patterns, we found significant patterns for both right and left Ext movement only in beta, gamma and HF bands. None or isolated EMG-EMG connections were found in alpha band. The highest IMC values were observed between target ED and FD for both left and right Ext. For all movements, IMC patterns in HF appeared to be less specific, i.e. involving all muscles.

As for right and left Grasp movements (Fig. 4), we found lower CMC values than in Ext. The EEG-EMG connections mainly involved the target muscle FD in alpha band, whereas ED and proximal muscles were involved in higher frequency bands. Similar to what observed for Ext, the involvement of bilateral sensorimotor areas characterized these CMC patterns. Like the Ext movement, the IMC patterns in both left and right grasping movement showed significant connections in beta, gamma and HF bands, with more muscles progressively involved at higher frequencies. A strong connection between ED and FD across these frequency bands is confirmed for Grasp movement executed with both left and right hand.

3.3. *Movement Classification*

Task-rest classification

The task-rest classification performances expressed as AUC, Accuracy, Specificity and Sensitivity are shown in Table 1. Overall, higher classification performances were observed for Ext with respect to Grasp, whereas performances are comparable between left and right movements.

The ANOVA on task-rest classification AUC revealed a significant effect of MOVEMENT ($F(1,16) = 13.16$, $p < 0.01$) and MOVEMENT × SIDE ($F(1,16) = 6.06$, $p = 0.03$) factors. No significant effect of the SIDE factor was observed ($F(1,16) = 0.19$, $p = 0.67$). The Tukey post-hoc analysis revealed significant differences ($p < 0.01$) between movements (Ext and Grasp) for both the right and the left side, as already suggested from the mean values in Table 1 (see Fig. A.1).

The analysis on selected features revealed that about 60 features were selected by the stepwise regression for each iteration and participant: 62 ± 3 ExtR, 64 ± 3 ExtL, 57 ± 3 GraspR, 52 ± 5 GraspL, presented as mean ± standard error. Figure 5 illustrates the most recurrent features across

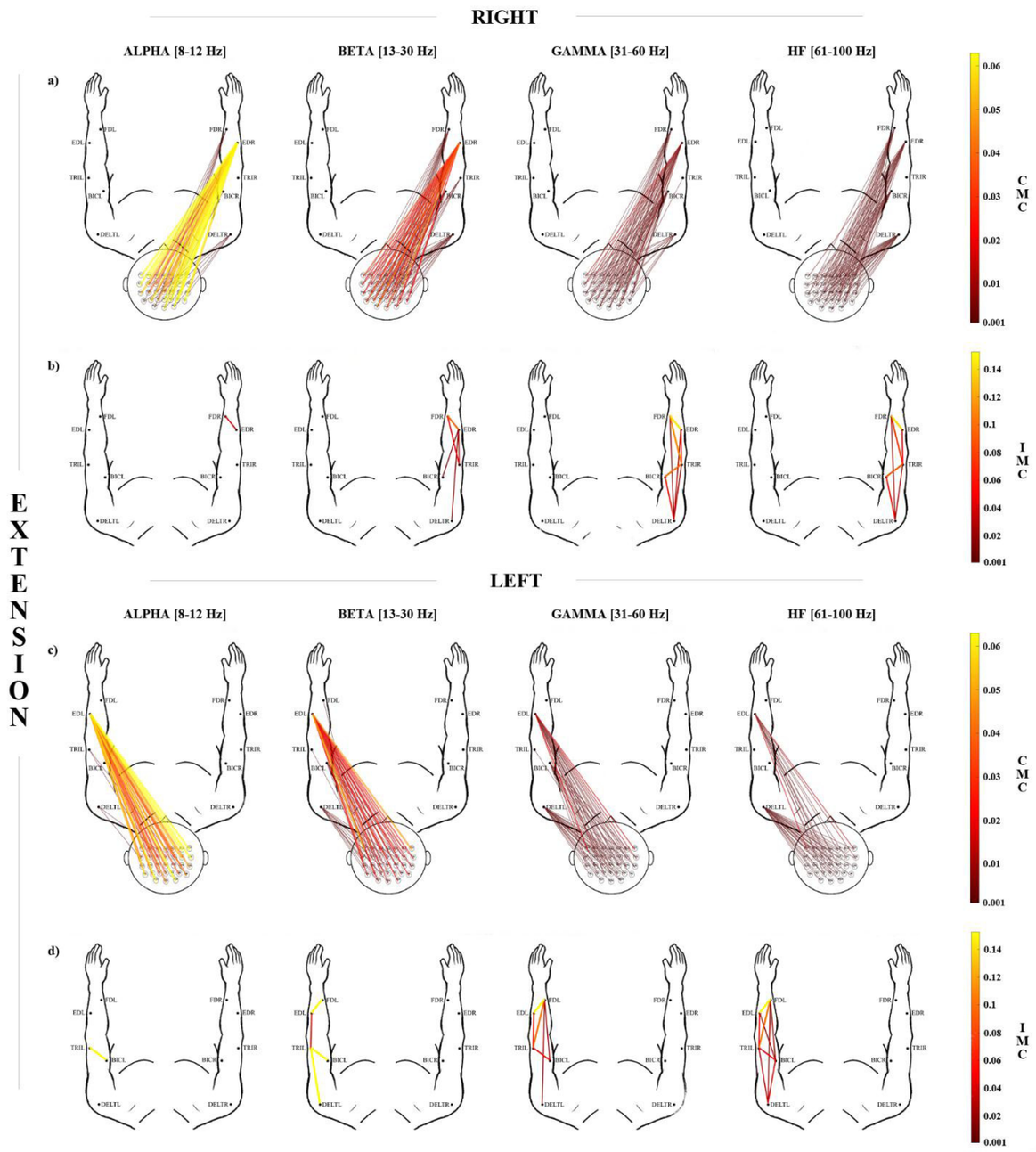

Fig. 3. Grand average coherence patterns during finger extension. Corticomuscular (CMC) and Intermuscular (IMC) patterns for the right finger extension movement (Ext) (panels (a) and (b) for CMC and IMC, respectively) and left Ext (panels (c) and (d) for CMC and IMC, respectively) and for each frequency band: alpha (8–12 Hz), beta (13–30 Hz), gamma (31–60 Hz) and high frequency, HF, band (61–100 Hz). The representation is seen from the above: scalp with nose pointing toward the top of the page and arms in front of the participant. Only statistically significant CMC/IMC values are represented (paired t-test between task and rest intervals, $\alpha = 0.05$ FDR correction). The color bar codes for the CMC/IMC average value (across participants, $N = 17$) in the task interval.

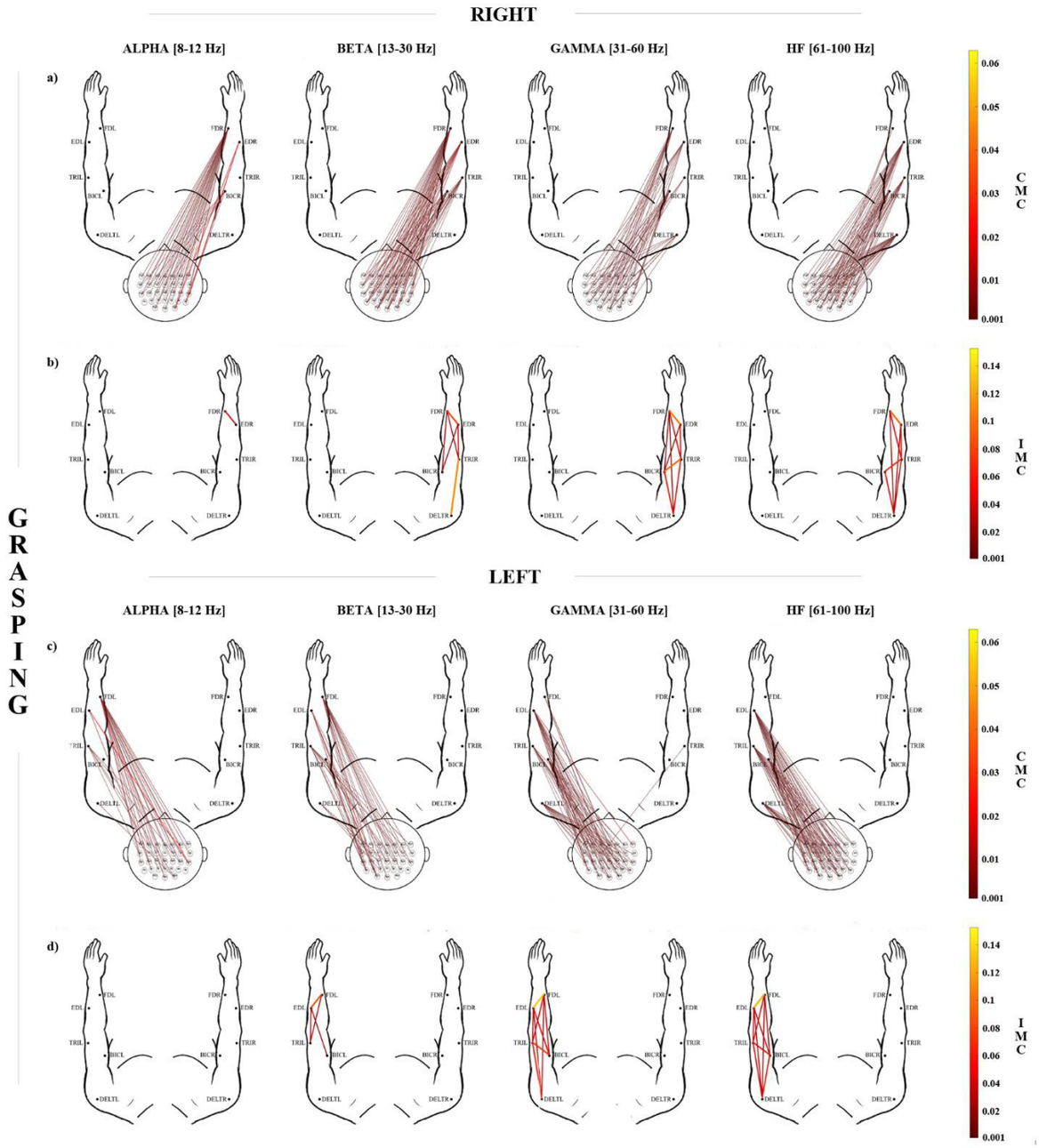

Fig. 4. Grand average coherence patterns during grasping. Corticomuscular (CMC) and Intermuscular (IMC) patterns for the right grasping movement (Grasp) (panels (a) and (b) for CMC and IMC, respectively) and left Grasp (panels (c) and (d) for CMC and IMC, respectively) and for each frequency band: alpha (8–12 Hz), beta (13–30 Hz), gamma (31–60 Hz) and high frequency, HF, band (61–100 Hz). The representation is seen from the above: scalp with nose pointing toward the top of the page and arms in front of the participant. Only statistically significant CMC/IMC values are represented (paired t-test between task and rest intervals, $\alpha = 0.05$ FDR correction). The color bar codes for the CMC/IMC average value (across participants, $N = 17$) in the task interval.

Table 1. Classification performances (AUC, Accuracy, Specificity and Sensitivity) of the CMC + IMC approach, reported as mean (standard error) across 17 participants, of the task-rest classifier. ExtR: finger extension with the right hand; ExtL: finger extension with the left hand; GraspR: grasping with the right hand; GraspL: grasping with the left hand.

Task versus Rest				
Movement	AUC	Accuracy	Specificity	Sensitivity
ExtR	0.95 (0.01)	0.90 (0.02)	0.95 (0.01)	0.85 (0.02)
ExtL	0.98 (0.01)	0.94 (0.01)	0.98 (0.01)	0.90 (0.01)
GraspR	0.89 (0.03)	0.82 (0.03)	0.86 (0.03)	0.79 (0.02)
GraspL	0.87 (0.02)	0.80 (0.02)	0.85 (0.03)	0.76 (0.02)

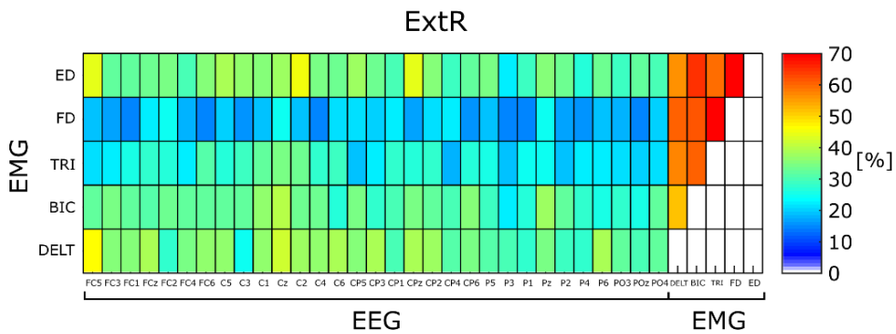

(a)

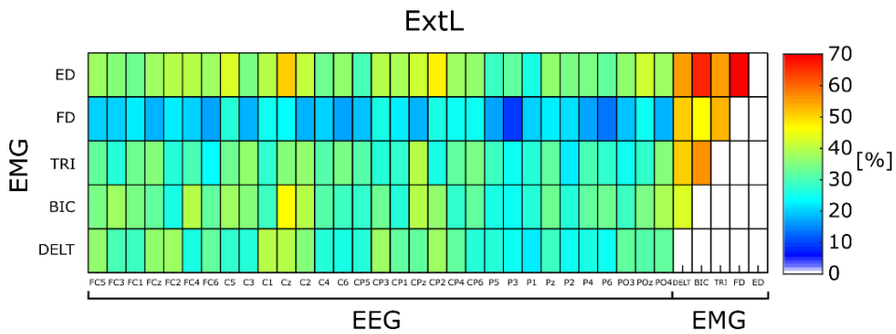

(b)

Fig. 5. Features selected in task versus rest classification. Most recurrent EEG-EMG pairs and EMG-EMG pairs selected by the stepwise regression across participants ($N = 17$) and cross-validation iterations (IT = 10) in the classification of each movement versus rest. The matrix shows for each EEG-EMG pair and EMG-EMG pair the number of times, expressed as percentage, each pair was selected over all participants and all iterations of the cross-validation. EEG-EMG pairs are identified by boxes from the intersection of EEG channels on the x-axis and EMG channels on the y-axis. EMG-EMG pairs are identified by boxes from the intersection of EMG channels on the x-axis and EMG channels on the y-axis. Panels (a) ExtR: finger extension with right hand, (b) ExtL: finger extension with left hand, (c) GraspR: grasping with right hand, (d) GraspL: grasping with left hand.

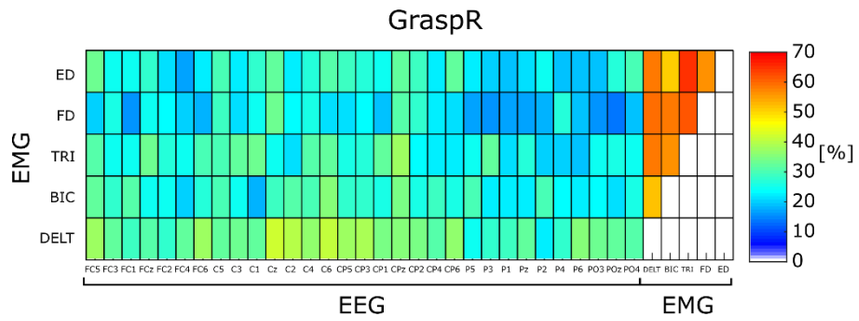

(c)

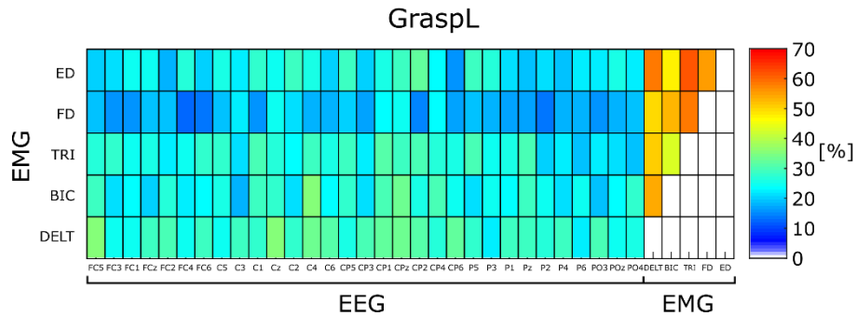

(d)

Fig. 5. (*Continued*)

participants ($N = 17$) and cross-validation iterations (IT = 10). For Ext movements, the IMC feature between the extensor digitorum muscle and the flexor digitorum muscle resulted the most recurrent (∼70%). As for the type of movements, CMC features involving the extensor digitorum muscle were recurrent in Ext movement. The CMC features involving distal (extensor and flexor digitorum muscles) as well as proximal muscles were selected in the Grasp movement, thus indicating a less "muscle-specific" selection for Grasp with respect to Ext movement. The CMC features mostly involved the central and centro-parietal EEG channels strips bilaterally, including the midline electrodes. No clear lateralization of CMC patterns (i.e. involvement of EEG electrode position contralateral to the movement) was found, except for ExtL (CP2 with the extensor digitorum muscle).

The same classification approach was applied separately for CMC and IMC features. The one-way repeated measures ANOVA on AUC, applied to test differences among types of features (CMC + IMC, CMC, IMC), revealed significant lower performance for IMC features in each of the four movements,

Table 2. Results of the one-way repeated measure ANOVA on AUC considering as independent variables the type of features (CMC + IMC, CMC and IMC) for each movement. The last three columns show the results of the Tuckey post-hoc analysis, — no significant differences, ** significance differences ($p < 0.01$).

Movement	F(p)	CMC + IMC versus CMC	CMC + IMC versus IMC	CMC versus IMC
ExtR ($df = 2, 32$)	26.86 (<0.01)	—	**	**
ExtL ($df = 2, 32$)	22.37 (<0.01)	—	**	**
GraspR ($df = 2, 32$)	43.59 (<0.01)	—	**	**
GraspL ($df = 2, 32$)	57.29 (<0.01)	—	**	**

as shown in Table 2. We did not observe significant differences between CMC and CMC + IMC features. The following classification performances for the three types of features were achieved: 0.92 (0.01) for CMC + IMC, 0.92 (0.01) for CMC and 0.74 (0.02) for IMC, presented as mean AUC (standard error) across movements.

Ext-Grasp classification

The ability of CMC and IMC features to discriminate between Ext and Grasp movements was tested with the same approach used to classify each movement versus rest. The Ext-Grasp classification performances expressed as AUC, Accuracy, Specificity and Sensitivity are shown in Table 3.

Table 3. Classification performances (AUC, Accuracy, Specificity and Sensitivity), reported as mean (standard error) across 17 participants, Ext-Grasp classifier.

Ext versus Grasp				
Side	AUC	Accuracy	Specificity	Sensitivity
Right hand	0.98 (<0.01)	0.95 (0.01)	0.95 (0.01)	0.95 (0.01)
Left hand	0.99 (<0.01)	0.95 (0.01)	0.96 (0.01)	0.95 (0.01)

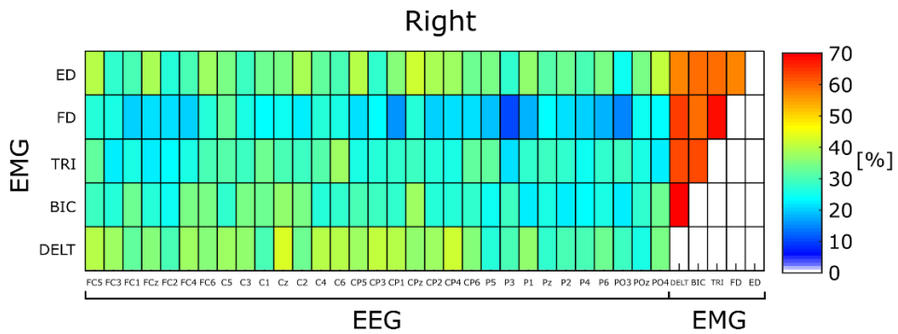

(a)

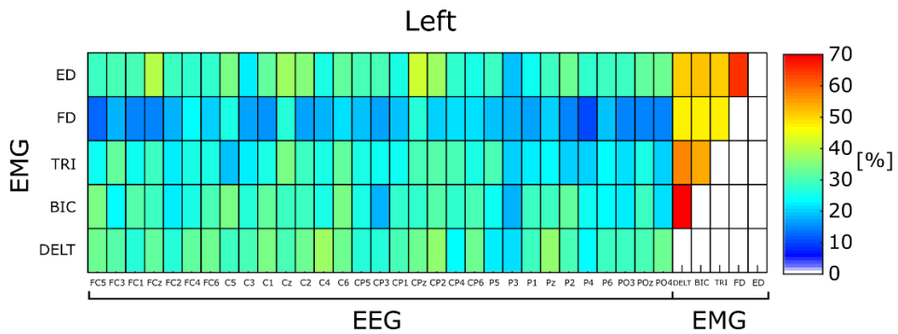

(b)

Fig. 6. Features selected in Ext versus Grasp classification. Most recurrent EEG-EMG pairs and EMG-EMG pairs selected by the stepwise regression across participants ($N = 17$) and cross-validation iterations (IT = 10) in the classification of finger extension versus grasping for each side. The matrix shows for each EEG-EMG pair and EMG-EMG pair the number of times, expressed as percentage, each pair was selected over all participants and all iterations of the cross-validation. EEG-EMG pairs are identified by boxes from the intersection of EEG channels on the x-axis and EMG channels on the y-axis. EMG-EMG pairs are identified by boxes from the intersection of EMG channels on the x-axis and EMG channels on the y-axis. Panels: (a) Right hand movements, (b) Left hand movements.

Table 4. Results of the one-way repeated measure ANOVA on AUC considering as independent variables the type of features (CMC + IMC, CMC and IMC) for each side. The last three columns show the results of the Tuckey post-hoc analysis, — no significant differences, ** significance differences ($p < 0.01$).

Side	F(p)	CMC + IMC versus CMC	CMC + IMC versus IMC	CMC versus IMC
Right (d$f = 2, 32$)	16.91 (<0.01)	—	**	**
Left (d$f = 2, 32$)	22.04 (< 0.01)	—	**	**

The paired t-test on Grasp-Ext classification AUC values did not reveal any significant effect of the SIDE ($t = 0.77$, $p = 0.45$). The analysis on selected features revealed that about 60 features were selected by the stepwise regression for each iteration and participant: 64 ± 3 ExtR-GraspR, 55 ± 5 ExtL-GraspL, presented as mean ± standard error. Figure 6 illustrates the most recurrent features across participants ($N = 17$) and cross-validation iterations (IT = 10). The CMC features mostly involved the central and centro-parietal EEG channels strips bilaterally, including the midline electrodes. No clear lateralization of CMC patterns (i.e. involvement of EEG electrode position contralateral to the movement) was found.

The same classification approach was applied separately for CMC and IMC features. The one-way repeated measures ANOVA on AUC, applied to test differences among types of features (CMC + IMC, CMC, IMC), revealed significant lower performance for IMC features in the task Ext versus Grasp executed with the right and the left side, as shown in Table 4.

We did not observe significant differences between CMC and CMC + IMC features. The following classification performances for the three types of features were achieved: 0.98 (<0.01) for CMC + IMC, 0.98 (<0.01) for CMC and 0.85 (0.02) for IMC, presented as mean AUC (standard error) across sides.

4. Discussion

In this study, we identified corticomuscular and intermuscular synchronization patterns (CMC and IMC) derived from EEG/EMG multichannel recording performed during the execution of simple hand movements (Ext and Grasp) in a sample of healthy participants. The finger extension and grasping movements could be distinguished by using the combination of CMC and IMC with better (offline) classification performances for the Ext with respect to Grasp movement. Furthermore, such combined CMC + IMC features allowed for successful classification of Ext versus Grasp. All in all, these findings represent a first step in designing novel hybrid BCI systems which better cope with central and peripheral drive of functional motor recovery after stroke.

CMC patterns characterization

The CMC grand average patterns showed significant connections between the whole sensorimotor areas and the muscles of the limb involved in the movement in the entire frequency range from alpha to gamma bands. This is in line with previous studies identifying beta as the typical band for CMC and alpha and gamma bands as reflecting feedback and feed-forward EEG-EMG interaction, respectively.[52]

Focusing on the distribution of those connections on the scalp, we noticed that the sensorimotor areas bilaterally concurred to the pattern regardless of the side and type of movement performed. Indeed, a prevalent activation of the contralateral sensorimotor cortex during upper limb movements would be expected according to common anatomical and physiological knowledge.[53] This lateralized cortical activation has been widely described in several EEG[54–56] and CMC studies.[26,28,57] Nevertheless, the active contribution of the ipsilateral motor cortex was described to have a facilitatory role in the control of the moving limb.[58]

It is well-known that movement preparation and execution is associated to an event-related desynchronization (ERD) which is an oscillatory phenomenon occurring within motor-related EEG frequency bands.[59] While ERD is highly lateralized (i.e. occurs mainly on the sensorimotor areas

contralateral to the movement) at movement onset, it has been described to evolve bilaterally on the scalp as movement progresses.[60,61] In our paradigm, participants were explicitly asked to perform Ext and Grasp movement slowly (for 4 s) and the time window for coherence analysis was defined as to start one second after the actual movement onset (see Fig. 1). It could be hypothesized that the bilateral involvement of the scalp sensorimotor areas in CMC patterns observed in our experimental condition would reflect the progression in time of the execution of the movements. It remains to be elucidated whether such bilateral scalp involvement will be confirmed in stroke subjects[30] and how this will impact on appropriate CMC features selection in a rehabilitative hybrid BCI setting.

Regarding the muscle-specificity of the observed CMC patterns, we found a central role of the agonist muscle (ED) during Ext movement, especially with the non-dominant hand. This observation was consistent with the task versus rest classification finding wherein the ED connections were the most recurrently selected among EEG-EMG pairs (see Fig. 5). The observed difference between dominant and non-dominant hand patterns did not affect task versus rest classification performances, which achieved around 90% for both ExtR and ExtL.

Grand average CMC patterns during Grasp movement showed lower CMC values than those obtained for Ext. This finding could reflect a certain degree of the inter-individual variability in performing the grasping movement that could be attributed to the wide spectrum of functional and behavioral correlates of the grasping movement.[62] In a previous study on healthy participants, we found that motor imagery of grasping movement was characterized by behavioral differences among individuals which significantly impacted on EEG sensorimotor reactivity.[63] The CMC patterns of Grasp showed less muscle-specificity (with respect to Ext). This finding is consistent with that observed for task versus rest classification where no muscle among the EEG-EMG pairs appeared more frequently selected than others (see Fig. 5).

IMC patterns characterization

As for IMC pattern representation, we found significant differences across frequency bands. Specifically, IMC patterns appeared to be more movement-specific in beta and gamma bands whereas unconnected and fully connected IMC patterns were observed in the alpha and HF band, respectively. Overall, these findings are in line with previous evidence[32] showing that IMC in alpha encodes for postural and subcortical control whose relevance is likely marginal in our paradigm (simple hand movements executed by healthy participants), while beta and gamma bands reflect cortical control on movement execution.[31,47,64,65]

Among EMG-EMG pairs, the connection between ED and FD muscles (i.e. the agonist/antagonist and antagonist/agonist for the Ext and Grasp movements, respectively), resulted to be the strongest in our IMC patterns, confirming findings of Kamper and colleagues.[47] The occurrence of spasticity and pathological co-contraction after stroke results in weakening of the agonist–antagonist coupling.[47] For this reason, the ED-FD synchronization will likely be a crucial feature for the implementation of our hybrid BCI paradigm for stroke subjects' rehabilitation. Nevertheless, the analysis of the features selected by the offline classification model to recognize each movement showed that connections involving the muscles other than ED and FD were also recurrent among healthy participants (e.g. biceps brachii in Grasp). This finding supports our methodological approach of acquiring information from multiple muscles (i.e. not limited to the forearm muscles) as necessary for the accurate classification of different hand movements. This will be especially true in the case of stroke subjects, where movement is often characterized by abnormal muscular activations (motor overflow, agonist–antagonist co-contractions) whose occurrence we should be capable of monitoring and discouraging.

Movement classification

Classification results revealed high performance of CMC/IMC features in discriminating each task against rest. Lower classification performances were, however, observed for the Grasp movement with respect to Ext. This finding is consistent with higher intra-individual variability for the Grasp already highlighted by the observation of CMC and IMC patterns. Again, a possible explanation for this could be found in the complexity of behavioral and functional implications of the grasping movement with

respect to finger extension.[62,63] Overall, our classification performances are higher than those reported in similar studies,[66] and this is especially true for the Ext movement. Of note, finger extension, and more generally extension movements are commonly employed in the rehabilitation of stroke subjects, especially when effectors such as robots or functional electrical stimulation are employed,[5,67,68] to contrast the common pathological flexion synergy of the upper limb.[69]

To further evaluate the movement specificity of CMC and IMC features we tested their ability to classify Ext versus Grasp in the dominant and non-dominant upper limb. Performances were again very high for both sides. The ability to non-invasively decode different types of movement is potentially interesting to achieve the so-called "natural control" of neuroprostheses,[70] which is an emerging issue in the field of BCIs for clinical applications beyond stroke (e.g. control of hand neuroprostheses after spinal cord injury[71]).

In all conditions (task versus rest and Ext versus Grasp), our hybrid approach did not outperform the classification results obtained by CMC alone, while both CMC and hybrid were significantly better than IMC. However, we would like to stress the fact that we included IMC in our paradigm with the aim to monitor the quality of movement rather than that of improving classification performances. Indeed, in our application for post-stroke rehabilitation, we want to reinforce only those movement attempts resembling physiological movement patterns.

Conclusion, limitations and future steps

Our findings on CMC and IMC obtained from healthy participants support the validity of the elements of novelty proposed in our paradigm. First, the conception of a hybrid BCI which includes EEG and EMG derived features encoding for physiological movement patterns (beyond the mere pursue of higher classification rates, yet showing satisfying performances). Second, the use of multiple EEG electrodes and EMG from several muscles bilaterally to compute CMC and IMC, in compliance with the literature showing that post-stroke changes may involve brain areas distant from the lesion and muscles other than the target ones. The characterization of such CMC/IMC patterns in a population of stroke subjects is lacking in this study and it requires the implementation of future investigations aiming at (i) defining how interactions between central and peripheral nervous systems are altered after stroke and (ii) providing new potential neurophysiological markers for post-stroke motor impairment and recovery along the rehabilitative process.

Furthermore, an additional limitation of the hybrid BCI system is that it requires recordable EMG from upper limb muscles, hence individuals with complete upper limb paralysis (i.e. plegia) may not be candidates for this BCI approach. Future studies on patients are needed to identify those that would benefit most of the proposed approached based on the amount and characteristics of their residual upper limb movements. Altogether, we are confident on the overall applicability of our approach to stroke patients basing on the recent findings, showing possibility to detect EMG activity even in severely impaired patients[20,72] and applicability of the CMC feature in a BCI context.[36]

Despite the promising findings reported in this study, further investigations are needed to evaluate the feasibility of real-time extraction of CMC and IMC-based features suitable to control a hybrid BCI system. The proposed multi-channel approach including signals from the whole sensorimotor areas and both upper limb muscles has been useful to comprehensively describe each simple movement by means of a CMC/IMC pattern highly discriminable against rest. However, this approach could hardly be translated as it is in an online BCI paradigm. To cope with this computational issue, we intend to reduce the complexity of such multi-channel analysis by selecting the best individual hybrid features for each task (e.g. few EEG-EMG/EMG-EMG channels pairs in specific frequency bands) to eventually be implemented online for a real-time control of a hybrid BCI.

Acknowledgment

This work was supported by the Italian Ministry of Health (Ricerca Corrente IRCCS Fondazione Santa Lucia, GR-2018-12365874 and RF-2018-12365210), by Sapienza University of Rome — Progetti di Ateneo 2020 (RM120172B8899B8C, AR220172B9222800, AR120172B8B5B405) and by the Promobilia Foundation (2018-H1 ref. 18076). We thank M. Rossi for his support in EMG data collection.

Appendix A

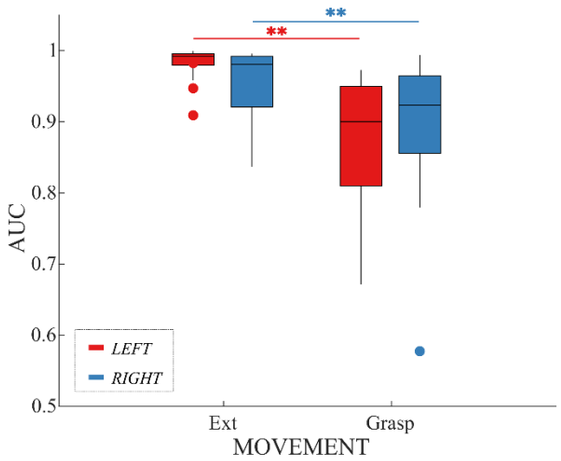

Fig. A.1. Distribution of task-rest classification performance. Boxplot of the distributions ($N = 17$ participants) of the Area Under the Receiver Operating Characteristic Curve (AUC) values for each movement (Ext, finger extension, and Grasp, grasping) executed with either hand (right and left). A single-subject 10-iteration cross-validation with a support vector machine classification model was implemented to classify each movement versus rest. Before training the classifier, stepwise regression-based feature selection was applied to reduce the dimension of the feature domain. The boxplot offers a complementary view of the results presented in the *paragraph task-rest classification* of *Movement Classification*. Markers (**) indicate significant differences ($p < 0.01$) between groups resulting from the Tukey post-hoc test. Significant differences were observed between movements, with higher performance in Ext movement classification. The intra-group variability, expressed as interquartile range of each AUC distribution, is higher for the grasping (0.14 and 0.11 for left and right grasping, respectively) than for extension (0.02 and 0.07 for left and right finger extension, respectively). Differences between sides were not significant.

References

1. M. A. Cervera, S. R. Soekadar, J. Ushiba, J. D. R. Millán, M. Liu, N. Birbaumer and G. Garipelli, Brain–computer interfaces for post-stroke motor rehabilitation: A meta-analysis, *Ann. Clin. Transl. Neurol.* **5** (2018) 651–663.
2. E. Monge-Pereira, F. Molina-Rueda, F. M. Rivas-Montero, J. Ibáñez, J. I. Serrano, I. M. Alguacil-Diego and J. C. Miangolarra-Page, Electroencephalography as a post-stroke assessment method: An updated review, *Neurologia* **32**(1) (2017) 40–49.
3. J. A. Barios, S. Ezquerro, A. Bertomeu-Motos, M. Nann, Fco. J. Badesa, E. Fernandez, S. R. Soekadar and N. Garcia-Aracil, Synchronization of slow cortical rhythms during motor imagery-based brain–machine interface control, *Int. J. Neur. Syst.* **29**(5) (2019) 1850045.
4. F. Pichiorri, G. Morone, M. Petti, J. Toppi, I. Pisotta, M. Molinari, S. Paolucci, M. Inghilleri, L. Astolfi, F. Cincotti and D. Mattia, Brain–computer interface boosts motor imagery practice during stroke recovery, *Ann. Neurol.* **77**(5) (2015) 851–865.
5. A. Biasiucci, R. Leeb, I. Iturrate, S. Perdikis, A. Al-Khodairy, T. Corbet, A. Schnider, T. Schmidlin, H. Zhang, M. Bassolino, D. Viceic, P. Vuadens, A. G. Guggisberg and J. d R. Millán, Brain-actuated functional electrical stimulation elicits lasting arm motor recovery after stroke, *Nature Publishing Group* **9**(1) (2018) 2421.
6. J. J. Daly and J. R. Wolpaw, Brain–computer interfaces in neurological rehabilitation, *Lancet Neurol.* **7**(11) (2008) 1032–1043.
7. F. Pichiorri and D. Mattia, Brain–computer interfaces in neurologic rehabilitation practice, in *Handbook of Clinical Neurology*, Vol. 168 (Elsevier, Amsterdam, 2020), pp. 101–116.
8. A. Ortiz-Rosario and H. Adeli, Brain–computer interface technologies: From signal to action, *Rev. Neurosci.* **24**(5) (2013) 537–552.
9. S. H. George, M. H. Rafiei, A. Borstad, H. Adeli and L. V. Gauthier, Gross motor ability predicts response to upper extremity rehabilitation in chronic stroke, *Behav. Brain Res.* **333** (2017) 314–322.
10. Y.-T. Chen, S. Li, E. Magat, P. Zhou and S. Li, Motor overflow and spasticity in chronic stroke share a common pathophysiological process: Analysis of within-limb and between-limb EMG-EMG coherence, *Front. Neurol.* **9** (2018) 795.
11. J. P. Dewald, P. S. Pope, J. D. Given, T. S. Buchanan and W. Z. Rymer, Abnormal muscle coactivation patterns during isometric torque generation at the elbow and shoulder in hemiparetic subjects, *Brain* **118**(**Pt 2**) (1995) 495–510.
12. M. F. Levin, R. W. Selles, M. H. Verheul and O. G. Meijer, Deficits in the coordination of agonist and antagonist muscles in stroke patients: Implications for normal motor control, *Brain Res.* **853**(2) (2000) 352–369.
13. L. C. Miller and J. P. A. Dewald, Involuntary paretic wrist/finger flexion forces and EMG increase with shoulder abduction load in individuals with chronic stroke, *Clin. Neurophysiol.* **123**(6) (2012) 1216–1225.
14. C. C. Silva, A. Silva, A. Sousa, A. R. Pinheiro, C. Bourlinova, A. Silva, A. Salazar, C. Borges, C. Crasto, M. V. Correia, J. P. Vilas-Boas and R. Santos, Co-activation of upper limb muscles during reaching in post-stroke subjects: An analysis of the contralesional and ipsilesional limbs, *J. Electromyogr. Kinesiol.* **24**(5) (2014) 731–738.
15. A. Chalard, D. Amarantini, J. Tisseyre, P. Marque and D. Gasq, Spastic co-contraction is directly

associated with altered cortical beta oscillations after stroke, *Clin. Neurophysiol.* **131**(6) (2020) 1345–1353.
16. J.-H. Park, J.-H. Shin, H. Lee, J. Roh and H.-S. Park, Alterations in intermuscular coordination underlying isokinetic exercise after a stroke and their implications on neurorehabilitation, *J. Neuroeng. Rehabil.* **18**(1) (2021) 110.
17. G. Müller-Putz, R. Leeb, M. Tangermann, J. Höhne, A. Kübler, F. Cincotti, D. Mattia, R. Rupp, K. Müller and J. d R. Millán, Towards noninvasive hybrid brain–computer interfaces: Framework, practice, clinical application, and beyond, *Proc. IEEE* **103**(6) (2015) 926–943.
18. A. Riccio, E. M. Holz, P. Aricò, F. Leotta, F. Aloise, L. Desideri, M. Rimondini, A. Kübler, D. Mattia and F. Cincotti, Hybrid P300-based brain-computer interface to improve usability for people with severe motor disability: Electromyographic signals for error correction during a spelling task, *Arch. Phys. Med. Rehabil.* **96**(3) (2015) S54–S61.
19. I. Choi, I. Rhiu, Y. Lee, M. H. Yun and C. S. Nam, A systematic review of hybrid brain-computer interfaces: Taxonomy and usability perspectives, *PLoS One* **12**(4) (2017) e0176674.
20. M. Kawakami, T. Fujiwara, J. Ushiba, A. Nishimoto, K. Abe, K. Honaga, A. Nishimura, K. Mizuno, M. Kodama, Y. Masakado and M. Liu, A new therapeutic application of brain-machine interface (BMI) training followed by hybrid assistive neuromuscular dynamic stimulation (HANDS) therapy for patients with severe hemiparetic stroke: A proof of concept study, *Restor. Neurol. Neurosci.* **34**(35) (2016) 789–797.
21. F. Grimm, A. Walter, M. Spüler, G. Naros, W. Rosenstiel and A. Gharabaghi, Hybrid neuroprosthesis for the upper limb: Combining brain-controlled neuromuscular stimulation with a multi-joint arm exoskeleton, *Front. Neurosci.* **10** (2016) 367.
22. E. Lóopez-Larraz, N. Birbaumer and A. Ramos-Murguialday, A hybrid EEG-EMG BMI improves the detection of movement intention in cortical stroke patients with complete hand paralysis, in 2018 40*th Annual Int. Conf. IEEE Engineering in Medicine and Biology Society* (*EMBC*) (Honolulu, HI, USA, 2018), pp. 2000–2003.
23. A. Sarasola-Sanz, N. Irastorza-Landa, E. López-Larraz, C. Bibián, F. Helmhold, D. Broetz, N. Birbaumer and A. Ramos-Murguialday, A hybrid brain–machine interface based on EEG and EMG activity for the motor rehabilitation of stroke patients, in 2017 *Int. Conf. Rehabilitation Robotics* (*ICORR*) (London, UK, 2017), pp. 895–900.
24. G. Morone, G. F. Spitoni, D. De Bartolo, S. Ghanbari Ghooshchy, F. Di Iulio, S. Paolucci, P. Zoccolotti and M. Iosa, Rehabilitative devices for a top-down approach, *Expert Rev. Med. Devices* **16**(3) (2019) 187–195.
25. A. Burns, H. Adeli and J. A. Buford, Upper limb movement classification via electromyographic signals and an enhanced probabilistic network, *J. Med. Syst.* **44**(10) (2020) 176.
26. T. Mima, K. Toma, B. Koshy and M. Hallett, Coherence between cortical and muscular activities after subcortical stroke, *Stroke* **32**(11) (2001) 2597–2601.
27. K. von Carlowitz-Ghori, Z. Bayraktaroglu, F. U. Hohlefeld, F. Losch, G. Curio and V. V. Nikulin, Corticomuscular coherence in acute and chronic stroke, *Clin. Neurophysiol.* **125**(6) (2014) 1182–1191.
28. L. H. Larsen, I. C. Zibrandtsen, T. Wienecke, T. W. Kjaer, M. S. Christensen, J. B. Nielsen and H. Langberg, Corticomuscular coherence in the acute and subacute phase after stroke, *Clin. Neurophysiol.* **128**(11) (2017) 2217–2226.
29. Z. Guo, Q. Qian, K. Wong, H. Zhu, Y. Huang, X. Hu and Y. Zheng, Altered corticomuscular coherence (CMCoh) pattern in the upper limb during finger movements after stroke, *Front. Neurol.* **11** (2020) 410.
30. R. Krauth, J. Schwertner, S. Vogt, S. Lindquist, M. Sailer, A. Sickert, J. Lamprecht, S. Perdikis, T. Corbet, J. del R. Millán, H. Hinrichs, H.-J. Heinze and C. M. Sweeney-Reed, Cortico-muscular coherence is reduced acutely post-stroke and increases bilaterally during motor recovery: A pilot study, *Front. Neurol.* **10** (2019) 126.
31. S. W. Lee, K. Landers and M. L. Harris-Love, Activation and intermuscular coherence of distal arm muscles during proximal muscle contraction, *Exp. Brain Res.* **232**(3) (2014) 739–752.
32. C. Charissou, D. Amarantini, R. Baurès, E. Berton and L. Vigouroux, Effects of hand configuration on muscle force coordination, co-contraction and concomitant intermuscular coupling during maximal isometric flexion of the fingers, *Eur. J. Appl. Physiol.* **117**(11) (2017) 2309–2320.
33. K. von Carlowitz-Ghori, Z. Bayraktaroglu, G. Waterstraat, G. Curio and V. V. Nikulin, Voluntary control of corticomuscular coherence through neurofeedback: A proof-of-principle study in healthy subjects, *Neuroscience* **290** (2015) 243–254.
34. D. C. Marquez, V. von Tscharner, K. Murari and B. M. Nigg, Development of a multichannel current-EMG system for coherence modulation with visual biofeedback, *Plos One* **13**(11) (2018) e0206871.
35. A. Ramos-Murguialday, D. Broetz, M. Rea, L. Läer, O. Yilmaz, F. L. Brasil, G. Liberati, M. R. Curado, E. Garcia-Cossio, A. Vyziotis, W. Cho, M. Agostini, E. Soares, S. Soekadar, A. Caria, L. G. Cohen and N. Birbaumer, Brain-machine interface in chronic stroke rehabilitation: A controlled study, *Ann. Neurol.* **74**(1) (2013) 100–108.
36. A. Chowdhury, H. Raza, Y. K. Meena, A. Dutta and G. Prasad, An EEG-EMG correlation-based brain-computer interface for hand orthosis supported

neuro-rehabilitation, *J. Neurosci. Methods* **312** (2019) 1–11.
37. G. Silasi and T. H. Murphy, Stroke and the connectome: How connectivity guides therapeutic intervention, *Neuron* **83**(6) (2014) 1354–1368.
38. N. Ejaz, J. Xu, M. Branscheidt, B. Hertler, H. Schambra, M. Widmer, A. V. Faria, M. D. Harran, J. C. Cortes, N. Kim, P. A. Celnik, T. Kitago, A. R. Luft, J. W. Krakauer and J. Diedrichsen, Evidence for a subcortical origin of mirror movements after stroke: A longitudinal study, *Brain* **141**(3) (2018) 837–847.
39. J. Tisseyre, D. Amarantini, A. Chalard, P. Marque, D. Gasq and J. Tallet, Mirror Movements are Linked to Executive Control in Healthy and Brain-injured Adults, *Neuroscience* **379** (2018) 246–256.
40. M. Barbero, R. Merletti and A. Rainoldi, *Atlas of Muscle Innervation Zones*: *Understanding Surface Electromyography and Its Applications* (Springer-Verlag, Mailand, 2012).
41. D. Stegeman and H. Hermens, Standards for suface electromyography: The European project Surface EMG for non-invasive assessment of muscles (SENIAM), **1** (2007).
42. A. Rainoldi, G. Galardi, L. Maderna, G. Comi, L. Lo Conte and R. Merletti, Repeatability of surface EMG variables during voluntary isometric contractions of the biceps brachii muscle, *J. Electromyogr. Kinesiol.* **9**(2) (1999) 105–119.
43. S. Rota, I. Rogowski, S. Champely and C. Hautier, Reliability of EMG normalisation methods for upper-limb muscles, *J. Sports Sci.* **31**(15) (2013) 1696–1704.
44. V. de Seta, J. Toppi, F. Pichiorri, M. Masciullo, E. Colamarino, D. Mattia, F. Cincotti, Towards a hybrid EEG-EMG feature for the classification of upper limb movements: Comparison of different processing pipelines, in 2021 10*th Int. IEEE/EMBS Conf. Neural Engineering* (*NER*), 2021, pp. 355–358.
45. T. Mima and M. Hallett, Corticomuscular coherence: A review, *Clin. Neurophysiol.* **16**(6) (1999) 501–511.
46. J. Bigot, M. Longcamp, F. Dal Maso and D. Amarantini, A new statistical test based on the wavelet cross-spectrum to detect time–frequency dependence between non-stationary signals: Application to the analysis of cortico-muscular interactions, *NeuroImage* **55**(4) (2011) 1504–1518.
47. D. G. Kamper, H. C. Fischer, M. O. Conrad, J. D. Towles, W. Z. Rymer and K. M. Triandafilou, Finger-thumb coupling contributes to exaggerated thumb flexion in stroke survivors, *J. Neurophysiol.* **111**(12) (2014) 2665–2674.
48. J. R. Rosenberg, A. M. Amjad, P. Breeze, D. R. Brillinger and D. M. Halliday, The Fourier approach to the identification of functional coupling between neuronal spike trains, *Prog. Biophys. Mol. Biol.* **53**(1) (1989) 1–31.
49. Y. Benjamini and D. Yekutieli, The control of the false discovery rate in multiple testing under dependency, *Ann. Stat.* **29**(4) (2001) 1165–1188.
50. J. O. Rawlings, S. G. Pantula and D. A. Dickey, A*pplied Regression Analysis*: *A Research Tool*, 2nd edn. (Springer-Verlag, New York, 1998).
51. T. Fawcett, An introduction to ROC analysis, *Pattern Recognit. Lett.* **27**(8) (2006) 861–874.
52. J. Liu, Y. Sheng and H. Liu, Corticomuscular coherence and its applications: A review, *Front. Hum. Neurosci.* **13** (2019) 1–16.
53. A. Nakamura, T. Yamada, A. Goto, T. Kato, K. Ito, Y. Abe, T. Kachi and R. Kakigi, Somatosensory homunculus as drawn by MEG, *NeuroImage* **7**(4) (1998) 377–386.
54. C. Toro, G. Deuschl, R. Thatcher, S. Sato, C. Kufta and M. Hallett, Event-related desynchronization and movement-related cortical potentials on the ECoG and EEG, *Electroencephalogr. Clin. Neurophysiol.* **93**(5) (1994) 380–389.
55. P. Ofner, A. Schwarz, J. Pereira and G. R. Müller-Putz, Upper limb movements can be decoded from the time-domain of low-frequency EEG, *PLoS One* **12**(8) (2017) e0182578.
56. A. Schwarz, M. K. Höller, J. Pereira, P. Ofner and G. R. Müller-Putz, Decoding hand movements from human EEG to control a robotic arm in a simulation environment, *J. Neural. Eng.* **17**(3) (2020) 036010.
57. T. Mima and M. Hallett, Electroencephalographic analysis of cortico-muscular coherence: Reference effect, volume conduction and generator mechanism, *Clin. Neurophysiol.* **110**(11) (1999) 1892–1899.
58. C. Rau, C. Plewnia, F. Hummel and C. Gerloff, Event-related desynchronization and excitability of the ipsilateral motor cortex during simple self-paced finger movements, *Clin. Neurophysiol.* **114**(10) (2003) 1819–1826.
59. G. Pfurtscheller and F. H. Lopes da Silva, Event-related EEG/MEG synchronization and desynchronization: Basic principles, *Clin. Neurophysiol.* **110**(11) (1999) 1842–1857.
60. C. Babiloni, F. Carducci, F. Cincotti, P. M. Rossini, C. Neuper, G. Pfurtscheller and F. Babiloni, Human movement-related potentials versus desynchronization of EEG alpha rhythm: A high-resolution EEG study, *NeuroImage* **10**(6) (1999) 658–665.
61. C. Neuper and G. Pfurtscheller, Event-related dynamics of cortical rhythms: Frequency-specific features and functional correlates, *Int. J. Psychophysiol.* **43**(1) (2001) 41–58.
62. A. I. Sburlea and G. R. Müller-Putz, Exploring representations of human grasping in neural, muscle and kinematic signals, *Nature Publishing Group* **8**(1) (2018) 16669.
63. F. Pichiorri, F. D. V. Fallani, F. Cincotti, F. Babiloni, M. Molinari, S. C. Kleih, C. Neuper, A. Kübler and D. Mattia, Sensorimotor rhythm-based

brain–computer interface training: The impact on motor cortical responsiveness, *J. Neural Eng.* **8**(2) (2011) 025020.

64. P. Brown and J. F. Marsden, Cortical network resonance and motor activity in humans, *Neuroscientist* **7**(6) (2001) 518–527.
65. J. A. Norton and M. A. Gorassini, Changes in cortically related intermuscular coherence accompanying improvements in locomotor skills in incomplete spinal cord injury, *J. Neurophysiol.* **95**(4) (2006) 2580–2589.
66. X. Lou, S. Xiao, Y. Qi, X. Hu, Y. Wang and X. Zheng, Corticomuscular coherence analysis on hand movement distinction for active rehabilitation, *Comput. Math. Methods Med.* **2013** (2013) 908591.
67. F. Quandt and F. C. Hummel, The influence of functional electrical stimulation on hand motor recovery in stroke patients: A review, *Exp. Transl. Stroke Med.* **6**(1) (2014) 9.
68. M. Gandolfi, N. Valè, E. K. Dimitrova, S. Mazzoleni, E. Battini, M. Filippetti, A. Picelli, A. Santamato, M. Gravina, L. Saltuari and N. Smania, Effectiveness of robot-assisted upper limb training on spasticity, function and muscle activity in chronic stroke patients treated with botulinum toxin: A randomized single-blinded controlled trial, *Front. Neurol.* **10** (2019) 41.
69. K. S. Sunnerhagen, A. Opheim and M. Alt Murphy, Onset, time course and prediction of spasticity after stroke or traumatic brain injury, *Ann. Phys. Rehabil. Med.* **62**(6) (2019) 431–434.
70. V. Mondini, R. J. Kobler, A. I. Sburlea and G. R. Müller-Putz, Continuous low-frequency EEG decoding of arm movement for closed-loop, natural control of a robotic arm, *J. Neural Eng.* **17**(4) (2020) 046031.
71. P. Ofner, A. Schwarz, J. Pereira, D. Wyss, R. Wildburger and G. R. Müller-Putz, Attempted arm and hand movements can be decoded from low-frequency EEG from persons with spinal cord injury, *Sci. Rep.* **9**(1) (2019) 7134.
72. A. Ramos-Murguialday, E. García-Cossio, A. Walter, W. Cho, D. Broetz, M. Bogdan, L. G. Cohen and N. Birbaumer, Decoding upper limb residual muscle activity in severe chronic stroke, *Ann. Clin. Transl. Neurol.* **2**(1) (2015) 1–11.